Reports of Practical Oncology and Radiotherapy 25 (2020) 109–112

Available online at www.sciencedirect.com

Reports of Practical Oncology and Radiotherapy

journal homepage: http://www.elsevier.com/locate/rpor

Original research article

Optimization of an ultra-fast silicon detector for proton and carbon beams using GEANT4 Monte Carlo toolkit

Mohsen Mashayekhi[a,*], Ali Asghar Mowlavi[a,b], Sayyed Bijan Jia[c], Hossein Ghayoumizadeh[d]

[a] Department of Physics, Hakim Sabzevari University, Sabzevar, Iran
[b] International Centre for Theoretical Physics (ICTP), Associate and Federation Schemes, Medical Physics Field, Trieste, Italy
[c] Department of Physics, University of Bojnord, Bojnord, Iran
[d] Department of Electrical Engineering, Vali-e-Asr University of Rafsanjan, Rafsanjan, Iran

ARTICLE INFO

Article history:
Received 18 December 2018
Received in revised form 5 November 2019
Accepted 18 December 2019
Available online 20 December 2019

Keywords:
Silicon detector
Energy cutoff
GEANT4 toolkit
Hadron therapy

ABSTRACT

Aim: The purpose of this study was to investigate the crosstalk effects between adjacent pixels in a thin silicon detector with 50 um thickness.
Background: There are some limitations in the applications of detectors in hadron therapy. So it is necessary to have a detector with concurrent excellent time and resolution. In this work, the GEANT4 toolkit was applied to estimate the best value for energy cutoff in the thin silicon detector in order to optimize the detector.
Materials and Methods: GEANT4 toolkit was applied to simulate the transport and interactions of particles. Calculations were performed for a thin silicon detector (2 cm × 2 cm×0.005 cm) irradiated by proton and carbon ion beams. A two-dimensional array of silicon pixels in the x-y plane with 100 um × 100 um × 50 um dimensions build the whole detector. In the end, the ROOT package is used to interpret and analyze the results
Results: It is seen that by the presence of energy cutoff, pixels with small deposited energy are ignored. The best values for energy cutoff are 0.01 MeV and 0.7 MeV for proton and carbon ion beams, respectively. By applying these energy cutoff values, efficiency and purity values are maximized and also minimum output errors are achieved.
Conclusions: The results are reasonable, good and useful to optimize the geometry of future silicon detectors in order to be used as beam monitoring in hadron therapy applications.

1. Background

Proton and carbon ion beam therapy is increasingly gaining acceptance in cancer treatment. In order to achieve ideal proton and carbon treatment outcomes, an accurate calculation of tissue stopping power is needed to estimate range and beam dose. But, currently, there are many unanswered questions regarding proton and carbon therapy.[1] One of the most important unknowns is the uncertainty in the position of the Bragg peak. The exact determination of the peak position is difficult due to internal motions of the patient organs during the treatment course.

Presently, precise tracking devices determine time quite poorly while good timing devices are too large for accurate position measurement.[2–4] This fact imposes severe limitations on the potential of many applications in medical treatments.[5–7] In order to obtain the high signal-to-noise ratio(S/N), it is necessary to have an ultra-fast detector. These fast sensors need to be very thin although the charge collected is reduced with respect to that of thicker sensors.[8–10] The combined spatial and timing precision is offered by ultra-fast silicon detector (UFSD). These fast detectors have applications in a whole array of different fields. For example, UFSD allows obtaining sharper images and monitor dose delivered in cancer treatment more accurately.[5] Also, these detectors are used to improve particle tracking in High-Energy physics experiments.

In this study, we have done Monte Carlo simulations of a thin silicon detector irradiated by Gaussian proton and carbon beams. We focused on the study of crosstalk effects between adjacent pixels in thin silicon detector with 50 um thickness.

* Corresponding author.
E-mail addresses: mmashayekhi1364@gmail.com (M. Mashayekhi), aa_Mowlavi@yahoo.com (A.A. Mowlavi), jiabijan@gmail.com (S.B. Jia), h.ghayoumizadeh@gmail.com (H. Ghayoumizadeh).

https://doi.org/10.1016/j.rpor.2019.12.020
1507-1367/

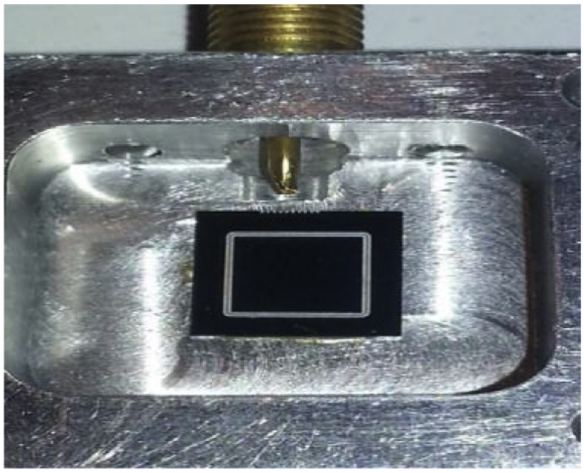

Fig. 1. UFSD sensors under study were produced by CNM (National Centre for Microelectronic) of Barcelona.

GEANT4 is a Monte Carlo code that is able to manage elementary particles and heavy ions interactions from threshold up to cosmic range energies. Simulations have been done by GEANT4 Monte Carlo toolkit version 4.10.01.[11]

2. Materials and methods

The simulations were performed using proton and carbon ion beams incident on the center of the silicon detector using the GEANT4 toolkit. The number of 4×10^6 incident particles were used in each set of the simulation. It is interesting for us to estimate energy distribution in the central axis of the detector and the probability of having particles in adjacent pixels around it. In addition, to minimize the effect of small energy released in the surrounding pixels, it is necessary to choose an appropriate energy cutoff.

Proton and carbon ion beams with Gaussian spatial distribution moving along the Z direction were assumed. The simulation was performed for different beam energies as 60, 100, 150, 250 MeV for protons and 150, 200, 300, 400 MeV/u for carbon ion beams. The detector is made of pure silicon with density of 2.33 g/cm^3.[12] The dimensions of the detector are $2 \times 2 \times 0.005$ cm^3 that is divided to 100 um pixels in the x-y plane. To evaluate the optimum detector thickness, different values were tested; the best was the 50 um thick detector. It is found that the full width at half maximum (FWHM) of the spatial distribution of incident beam does not have a significant effect on the results. Here we chose a value of 3 mm for FWHM as it is for the CNAO proton therapy facility. The standard package and binary cascade model have been used for EM and hadronic interactions, respectively.

The probability to select the pixels with higher deposited energy from all of the particles (primary and secondary) in the detector is defined as efficiency and probability to select only the pixel with higher deposited energy is defined as Purity. For data analysis, the ROOT package as an object-oriented framework[13] is used for analysis of the simulation outputs. By creating some macro files in ROOT, analysis for all events recorded in the detector were done separately. Fig. 1 shows a UFSD sensor that was produced by CNM.

3. Results

The efficiency and purity values for proton and carbon ion beams of different energies are listed in Tables 1 and 2, respectively. Table 1 contains the results for proton beam. In this table, first column shows the value for energy cutoff to ignore small energy deposited in adjacent pixels in the silicon detector. By applying energy cutoff, probability to select the pixels with higher energy (efficiency) and probability to select only the pixel with higher energy (Purity) are presented in the second and third columns. The statistic errors for all of outputs are listed, too.

In this study the best energy cutoff values for proton and carbon ion beams are 0.01 MeV and 0.7 MeV, respectively. This is important for us, that by applying an appropriate energy cutoff, the values of efficiency and purity are stable and maximum for different beamenergies (Fig. 2).

Fig. 3 shows a histogram that indicates energy distribution for each event in all of the detector pixels for 60 MeV proton beam. Energy distribution in one pixel and more than one pixel are presented in Figs. 4 and 5.

Table 1
Efficiency and purity values after applying energy cutoff for proton beam.

Energy cutoff (MeV)	Proton Energy (MeV/u)	Efficiency	Purity
0.01	60	0.9998 ± 0.0001	0.9764 ± 0.0001
	100	0.9999 ± 0.0009	0.9800 ± 0.0001
	150	0.9999 ± 0.0009	0.9836 ± 0.0001
	250	0.9998 ± 0.0001	0.9872 ± 0.0001
0.02	60	0.9998 + 0.0001	0.9807 + 0.0001
	100	0.9999 + 0.0009	0.9839 + 0.0001
	150	0.9998 + 0.0001	0.9869 + 0.0001
	250	0.9698 + 0.0001	0.9896 + 0.0001
0.03	60	0.9998 + 0.0001	0.9853 + 0.0001
	100	0.9998 + 0.0001	0.9875 + 0.0001
	150	0.9721 + 0.0001	0.9897 + 0.0001
	250	0.4579 + 0.0004	0.9853 + 0.0001
0.04	60	0.9998 + 0.0001	0.9898 + 0.0009
	100	0.9917 + 0.0009	0.9910 + 0.0009
	150	0.5983 + 0.0004	0.9891 + 0.0001
	250	0.1711 + 0.0003	0.9793 + 0.0003
0.05	60	0.9998 + 0.0001	0.9932 + 0.0008
	100	0.8031 + 0.0003	0.9923 + 0.0009
	150	0.2666 + 0.0004	0.9869 + 0.0002
	250	0.0876 + 0.0002	0.9791 + 0.0004
0.06	60	0.9986 + 0.0003	0.9956 + 0.0006
	100	0.4490 + 0.0004	0.9919 + 0.0001
	150	0.1393 + 0.0003	0.9875 + 0.0002
	250	0.0509 + 0.0002	0.9822 + 0.0005

Table 2
Efficiency and purity values after applying energy cutoff for carbon ion beams.

Energy cutoff (MeV)	Carbon Energy (MeV/u)	Efficiency	Purity
0.3	150	0.9996 + 0.0001	0.9993 + 0.0002
	200	0.9996 + 0.0001	0.9993 + 0.0002
	300	0.9997 + 0.0001	0.9993 + 0.0002
	400	0.9997 + 0.0001	0.9994 + 0.0002
0.4	150	0.9996 + 0.0001	0.9995 + 0.0002
	200	0.9996 + 0.0001	0.9995 + 0.0002
	300	0.9997 + 0.0001	0.9995 + 0.0002
	400	0.9997 + 0.0001	0.9995 + 0.0002
0.5	150	0.9996 + 0.0001	0.9996 + 0.0001
	200	0.9996 + 0.0001	0.9996 + 0.0001
	300	0.9997 + 0.0001	0.9996 + 0.0001
	400	0.9997 + 0.0001	0.9996 + 0.0001
0.6	150	0.9996 + 0.0001	0.9997 + 0.0001
	200	0.9996 + 0.0001	0.9997 + 0.0001
	300	0.9997 + 0.0001	0.9997 + 0.0001
	400	0.9997 + 0.0001	0.9997 + 0.0001
0.7	150	0.9997 ± 0.0001	0.9997 ± 0.0001
	200	0.9996 ± 0.0001	0.9997 ± 0.0001
	300	0.9997 ± 0.0001	0.9997 ± 0.0001
	400	0.9997 ± 0.0001	0.9997 ± 0.0001
0.8	150	0.9996 + 0.0001	0.9998 + 0.0001
	200	0.9996 + 0.0001	0.9998 + 0.0001
	300	0.9996 + 0.0001	0.9998 + 0.0001
	400	0.9652 + 0.0001	0.9998 + 0.0001

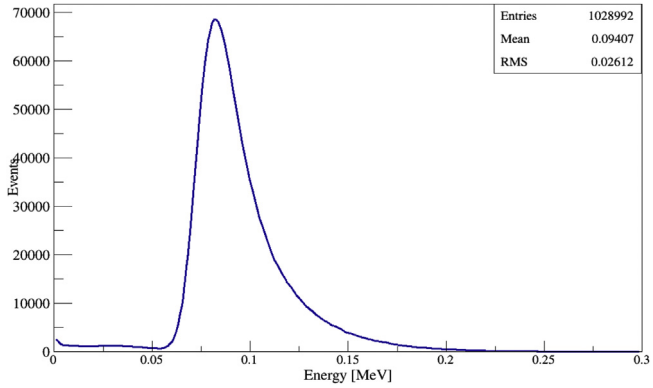

Fig. 2. Energy distribution in all of pixels for 60 MeV proton beam.

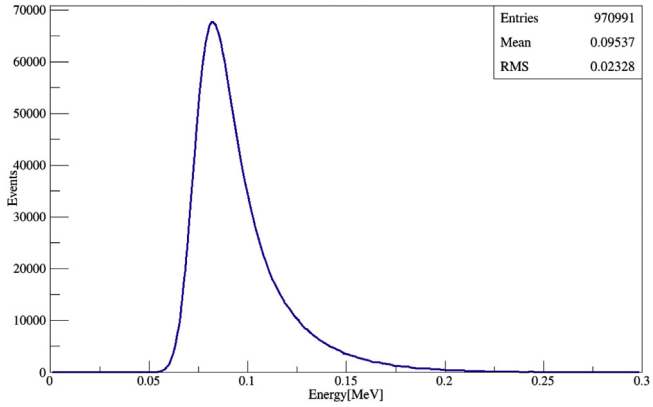

Fig. 3. Energy distribution in one pixel for 60 MeV proton beam.

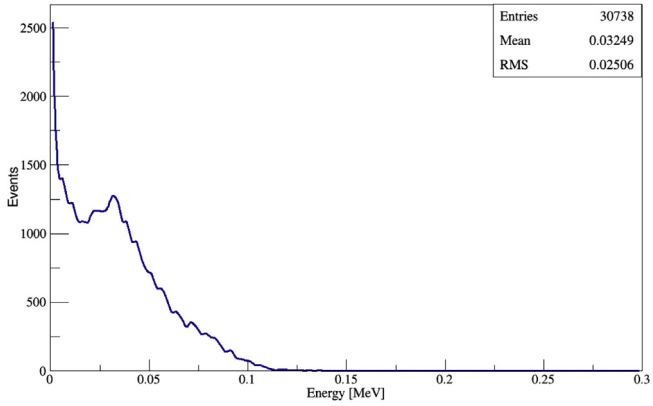

Fig. 4. Energy distribution in more than one pixel for 60 MeV proton beam.

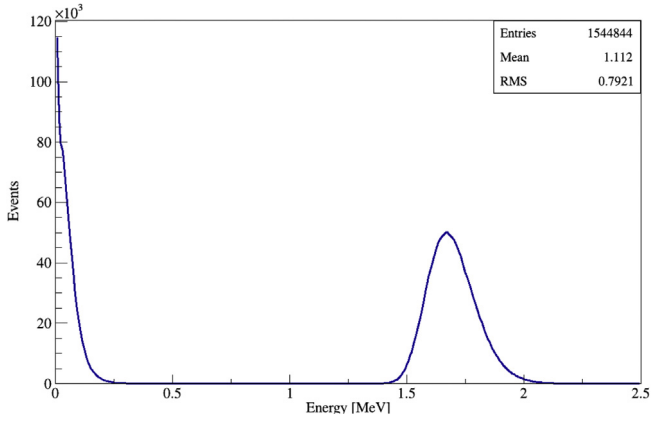

Fig. 5. Energy distribution in all of pixels for 150 MeV/u carbon ion beam.

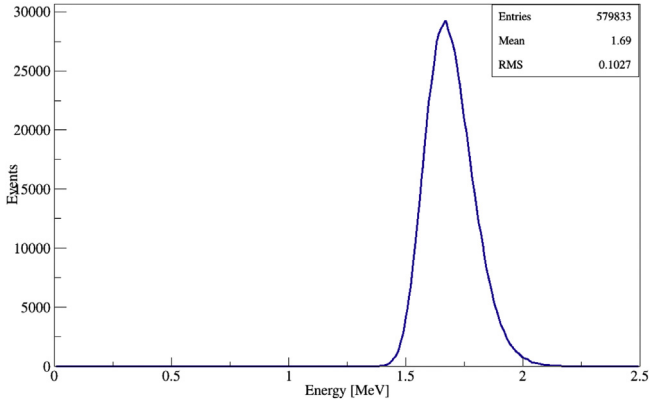

Fig. 6. Energy distribution in one pixel for 150 MeV/u carbon ion beam.

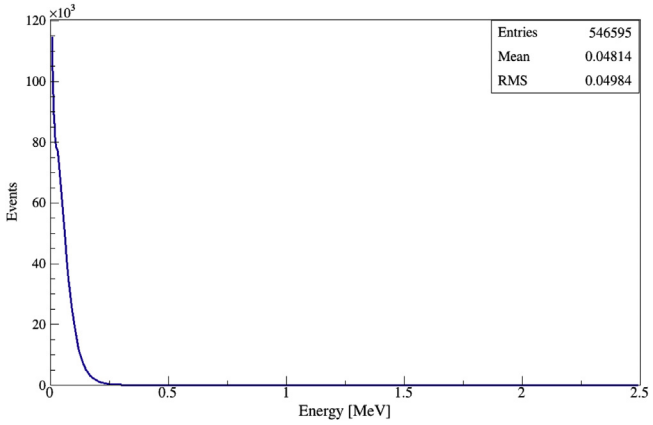

Fig. 7. Energy distribution in more than one pixel for 150 MeV/u carbon ion beam.

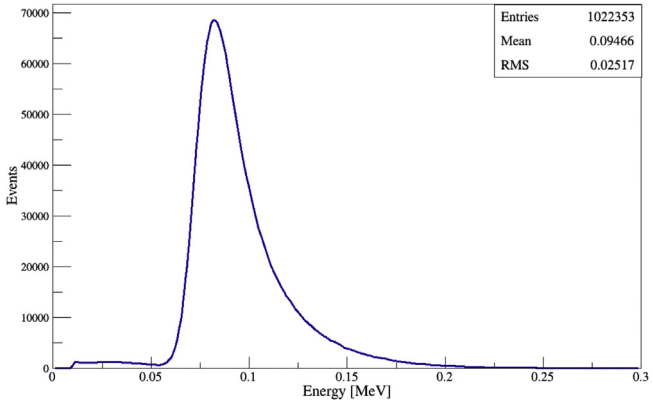

Fig. 8. Energy distribution in all of pixels for 60 MeV proton beam by applying energy cutoff.

Figs. 6–8 show the results for carbon ion beams for 150 MeV energy per nucleon. In these Figs the energy distribution is shown in all of the pixels, one pixel and more than one pixel, respectively. The values of entries, mean and the root mean square (RMS) are inserted as legends to each Fig (Fig. 9).

Here, we selected and presented only Figs for two states of proton and carbon ion beam energies, i.e, 60 and 150 MeV/u.

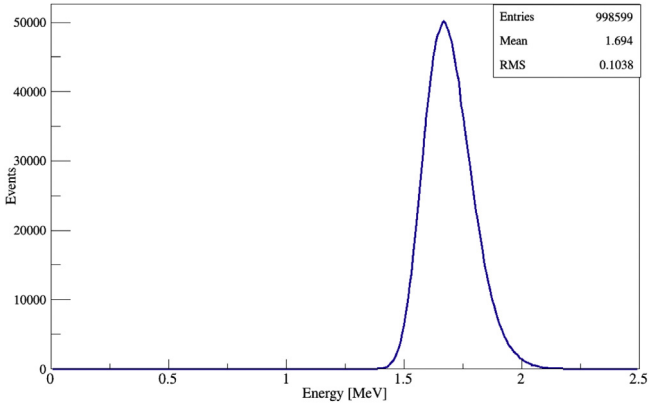

Fig. 9. Energy distribution in all of pixels for 150 MeV/u carbon ion beam by applying energy cutoff.

4. Discussions

Having the capability to determine the Bragg peak position with high precision can improve both the treatment planning procedure and beam delivery to the patient.

UFSD performance would allow us to develop new tools in single particle counting applications with unprecedented rate capabilities. For example, in hadron therapy, such a tool would measure the delivered dose to patients by directly counting the number of particles. By applying an energy cutoff, pixel with maximum energy deposition is considered and the rate of signal to noise will increase. This phenomenon helps us to obtain sharper image in order to monitor the delivered dose more accurately. Crosstalk is a leakage light produced in a matrix of silicon detector that affects spatial resolution. With the analysis of each pixel for each event, the best energy cutoff value is calculated.

In order to have just pixels with higher deposited energy, it is necessary to have an energy cutoff value for different beam energies; pixels with small energy will be ignored by applying the 0.01 MeV energy cutoff.

By applying a value of 0.7 MeV for energy cutoff, we can choose pixels with higher deposited energy and minimize the effect of small energy released in the surrounding pixels. Also, the best thickness for a thin silicon detector is 50 um and the results for this detector is better than one with 100 and 200 um thickness. The energy cutoff values for 100 um detector thickness are 0.04 and 1.3 MeV for proton and carbon beams, respectively. By applying this energy cutoff, the differences of efficiency and purity values compared to 50 um detector thickness would be very small and also the standard deviation of the obtained results is minimum.

5. Conclusion

We have proposed the development of a thin silicon detector in order to recover spatial resolution parameter. In this study, proton and carbon ion beams and also a thin silicon detector as a new monitoring system were simulated. By using GEANT4 Monte Carlo toolkit, energy deposition in the silicon detector was calculated. Data analysis for each pixel is determined by Root package. It can be seen, that by applying a proper value for energy cutoff we have pixels with higher energy without considering pixels with small energies. This phenomenon helps us to obtain a sharper image in order to monitor the delivered dose more accurately. Results are good and reasonable.

Conflict of interest

None declared.

Financial disclosure

None declared.

References

1. Lin L, Vargas C, Hsi W, et al. Dosimetric uncertainty in cancer proton radiotherapy. *Med Phys*. 2008;35:4800–4807.
2. Cartiglia N, Baselga M, Dellacasa G, et al. Performance of ultra-fast silicon detectors. *JINST*. 2014;9:C02001.
3. Sadrozinski Hartmut FW. Applications of silicon detectors. *IEEE Trans Nucl Sci*. 2001;48:933–940.
4. Bruzzi Sadrozinskin, Hartmut F-W, Seiden A. Comparing radiation tolerant materials and devices for ultra rad-hard tracking detectors. *Nucl Instrum Meth*. 2007;A579:754–761.
5. Sola V, Arcidiacono R, Bellora A, et al. Ultra-Fast silicon detectors for 4D tracking. *JINST*. 2017;12(02):C02072.
6. Spanoudaki VCh, Levin CS. Photo-detectors for time of flight positron emission tomography (ToF-PET). *Sensors*. 2010;10:10484–10505.
7. Hong SJ, Kang HG, Ko GB, et al. Si PM-PET with a short optical fiber bundle for simultaneous PET- MR imaging. *Phys Med Biol*. 2012;57:3869–3883.
8. RD50 Collaboration, http://rd50.web.cern.ch/rd50/.
9. Cartiglia N, Arcidiacono R, Bellora A, et al. The 4D pixel challenge. *JINST*. 2016;11(12):C12016.
10. Cartiglia N, Dellacasa G, Garbolino S, et al. Timing capabilities of ultra-fast silicon detector. *24th RD50 Workshop*. 2014:657.
11. Agostinelli S, Allison J, Amako K, et al. Geant4 — a simulation toolkit. *Nucl Instrum Meth A*. 2003;506:250–303.
12. *Geant4 material database*; 2015 http://geant4.web.cern.ch.
13. ROOT package. https://root.cern.ch/.